

Estimation of time-optimal control for two-level quantum system with bounded amplitude

Xikun Li^{1, 2}

¹*School of Physics and Optoelectronic Engineering, Anhui University, Hefei, Anhui 230601, China*

²*Max-Planck-Institut für Physik komplexer Systeme, D-01187 Dresden, Germany*

A systematic scheme is proposed to numerically estimate the quantum speed limit and temporal shape of time-optimal control. Two quantum state transitions in the two-level quantum system with constrained control field are studied as illustration. Comparisons between numerical results and analytical results are made, and deviations are significantly small. The shape of optimized control field is simple and does not switch frequently, thus are easy to implement in experiment. Our scheme is of importance in estimating the quantum speed limit and time-optimal controls in cases in which analytical solution is absent.

I. INTRODUCTION

Quantum optimal control (QOC) is crucial to engineer and to manipulate complex quantum systems in quantum information processing tasks [1–4]. Operations in experiments are generally executed very slowly, i.e., adiabatically, to avoid heating the sample and to guarantee the transition to the target state with perfect fidelity [5]. However, the decoherence and noise in experiments sometimes make such slow operations impossible, thus it is desirable to achieve a speedup in a fast and robust manner. This is one important topic of quantum optimal control theory [6, 7].

Quantum optimal control theory has been widely applied in various physical systems such as Bose-Einstein condensate [8], NMR [9], cold atoms in optical lattices [10, 11]. One of the core problems in QOC theory is to find the time-optimal control. Time-optimal control problems focus on driving transitions to the target states in the *minimal* time which is generally called the quantum speed limit (QSL) [12], and on finding the temporal shape of the control field. However, analytic solutions are only available for low-dimensional quantum systems [13]. For example, the analytic solutions are obtained for two-level system for energy minimization [14, 15] and time-optimal problems [16–23]. Therefore one has to perform numerical calculations when analytic solutions are not available.

For multiple-level quantum systems, in general, quantum optimal control relies on numerical methods, which employ local optimization algorithms, like Krotov [24], GRAPE [9], CRAB [25], GROUP [26] and GOAT [27], as well as global ones such as differential evolution (DE) and covariance matrix adaptation evolution strategy (CMA-ES) [10, 28], and reinforcement learning [29]. In experiments there might be constraints on the control field, e.g., the amplitude is bounded. In addition, the total duration is also limited for the time-optimal control problems. In such cases the local suboptimal traps exist in the quantum control landscape [30, 31]. These local traps make the numerical methods fail to find the global optimal solution, even with the global optimization algorithms. In addition, some methods cannot be applied in the prob-

lems where amplitude of control fields are bounded, while optimized controls found by some methods switch too frequently that are hardly possible to implement in real experiment.

In this paper we propose a systematic scheme to numerically estimate the quantum speed limit and time-optimal controls. As an illustration we investigate the time-optimal control problem for quantum state transitions in two-level quantum system with bounded amplitude. Analytical results are provided in Refs. [18]. We use the numerical scheme proposed, and compare the numerical results obtained to the analytical results. We find that the deviations from the analytical results are significantly small. Moreover, time-optimal controls obtained have simple shape, and do not switch frequently. This numerical scheme can be generalized to time-optimal control problems in multiple-level quantum systems in which the analytical solutions are absent.

II. MODEL

A. Hamiltonian

Here we consider a two-level quantum system driven by the controlled Hamiltonian described in the following:

$$H(t) = -E\sigma_z + \omega(t)\sigma_x = \begin{pmatrix} -E & \omega(t) \\ \omega(t) & E \end{pmatrix}, \quad (1)$$

where σ_z is the drift Hamiltonian and $E > 0$. The bounded control field $\omega(t)$ is a real function under constraint $|\omega(t)| \leq M$. When the control field is turned off, the lower (upper) eigenstate is $|0\rangle = \begin{pmatrix} 1 \\ 0 \end{pmatrix}$ ($|1\rangle = \begin{pmatrix} 0 \\ 1 \end{pmatrix}$). The dynamics of the system is governed by the controlled Hamiltonian $d|\psi(t)\rangle/dt = -iH(t)|\psi(t)\rangle$, where we set $\hbar = 1$.

One important parameter is defined as: $\alpha \equiv \arctan(M/E)$. It is easier to solve the problem of finding time-optimal control and quantum speed limit in the case $\alpha > \pi/4$ than that in the case $\alpha < \pi/4$ [18].

Therefore, we choose $E = 1$ and $M = 4/3$ such that $\alpha = 0.9273 > \pi/4$.

Numerically, for a quantum optimal control problem, we wish to optimize certain *fitness* functions such that the quantum speed limit T_{qsl} and optimized control field are obtained. The fitness function is a functional of control field $\omega(t)$, thus we are able to investigate the control landscape for certain types of control field. One common choice of fitness function is the fidelity between two quantum states. In our paper the fidelity is defined as follows:

$$\begin{aligned} F(\omega(t), T) &= |\langle \psi_t | \mathcal{T} \exp(-i \int_0^T H(t) dt) | \psi_i \rangle|^2 \quad (2) \\ &= |\langle \psi_t | \psi_f \rangle|^2. \end{aligned}$$

where \mathcal{T} is the time-ordering operator, and $|\psi_t\rangle$ ($|\psi_i\rangle$) is the target (initial) state. T is the total duration of time evolution, and $|\psi_f\rangle$ is the final state after the time evolution. An alternative characterising the similarity between the final state $|\psi_f\rangle$ and the target state $|\psi_t\rangle$ is the Bures distance

$$d_B = \sqrt{2(1 - |\langle \psi_f | \psi_t \rangle|)} = \sqrt{2(1 - \sqrt{F})}. \quad (3)$$

Perfect fidelity gives zero Bures distance, and vice versa.

We are interested in two transition processes with the bounded controls: (1) transition from $|0\rangle$ to $|1\rangle$; (2) transition from $|0\rangle$ to $|\psi_E\rangle$, where $|\psi_E\rangle = 1/\sqrt{2}(|0\rangle + e^{i9\pi/10}|1\rangle)$. We wish to estimate the quantum speed limit, as well as to determine the temporal shape of the time-optimal controls, of two transitions with the aid of numerical optimization over bang-off control fields defined in the following.

B. Bang-Off control

Inspired by Ref. [18] we consider the *bang-off* control as the control protocol to be optimized. For certain duration $[s, s + \delta s]$, if the control is restricted to take its maximum (minimum) $\omega(t) = M$ ($\omega(t) = -M$), it is called a *bang* control, and is denoted by $P_{\delta s}$ ($N_{\delta s}$), here P (N) is short for Positive (Negative); Similarly, if the value of control is zero $\omega(t) = 0$, it is called a *off* control, and is denoted by $0_{\delta s}$. Note that this is also called singular control [18]. The bang-off control refers to a finite concatenation of bang and off controls.

We consider two classes of bang-off control. For the first class the duration for bang/off controls is in general different, e.g., $P_{t_1} 0_{t_2} N_{t_3}$ defined in the following

$$\omega(t) = \begin{cases} M & 0 \leq t < t_1 \\ 0 & t_1 \leq t < t_1 + t_2 \\ -M & t_1 + t_2 \leq t \leq t_1 + t_2 + t_3, \end{cases} \quad (4)$$

where the order of letter sequence is from left to right. For the example above, the bang-off control is switched

from bang (P) to off (0), then to bang (N), with a switch number being two $N_s = 2$. The *type* of such bang-off controls refers to a way in which bang and off controls are concatenated. For a given number of switches N_s , the number of possible types N_{type} is at most 3×2^{N_s} . For certain initial/target quantum states, N_{type} can be further reduced. The control fields are represented by the type and vector of durations $\mathbf{t} = [t_1, t_2, \dots]$.

For the second class the duration of each bang/off is the time step-size: $\delta t = T/N_T$ with T being total duration and N_T the number of time slots. Thus the control is usually represented by a control vector $\omega(t) \equiv \{\omega_k | k = 1, \dots, N_T\}$. This class of bang-off control arises because of a coarse-graining of temporal variable for a numerical optimization. In general, the simulation is more accurate when N_T is larger. However, the optimization with large N_T is time-consuming, and the dimension of search space is huge. For the problems considered here the control is allowed to take 3 different values $\omega_k = \{\pm M, 0\}$, thus the possible number of control vectors is 3^{N_T} , which is an exponentially large number. For the quantum optimal control problem of two-level system, N_s is much smaller than N_T in general. Thus the optimization of first class of bang-off controls is much easier than that of second one. In addition, the optimized controls of second class generally switch more frequently than the ones of first class, thus are less desirable in real experiments.

Note that we do not claim that the first class of bang-off control is time-optimal control protocol for *all* QOC problems, e.g., time-optimal control of nonlinear two-level quantum system [7]. Instead, we use the first class of bang-off control to *estimate* QSL and to *approximate* the temporal shape of time-optimal control. This is due to the fact that the shape of first class of bang-off control is simple and its universality is in general better than bang-bang control. In addition, the optimality of first class of bang-off control has been proved in the two-level Landau-Zener system [18]. Therefore, we mainly focus on the study of first class of bang-off control.

C. Optimization algorithm

Optimization algorithms are of great importance for quantum optimal control problems. Here we use stochastic descent (SD) as the optimization algorithm [29]. Stochastic descent, a gradient-free algorithm, starts from a random configuration and updates control field $\omega(t)$ only if the candidate increases (decreases) the fidelity (Bures distance).

The reason for using SD is two-fold: first, SD is one of the simplest optimization algorithm. It could serve as a benchmark for comparing with other sophisticated algorithms; second, as we will see in the next sections, the control landscape is, in general, very flat over a large domain of controls when fidelity is approaching one $F \approx 1$. Therefore, the gradient-based algorithms in general stop updating because the gradient becomes exponentially

III. TRANSITION FROM $|0\rangle$ TO $|1\rangle$

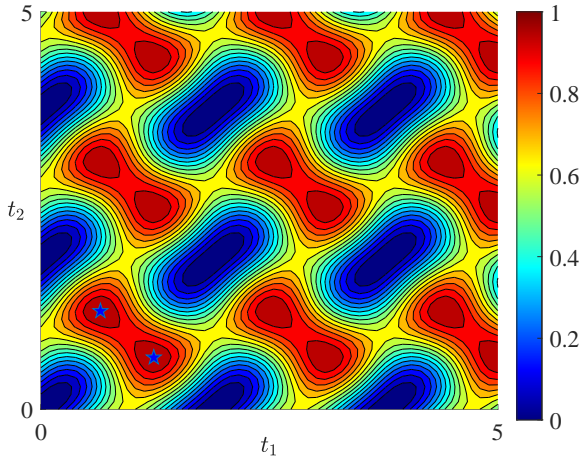


FIG. 1. Quantum control landscape of fidelity F for type $P_{t_1}N_{t_2}$ of the first class bang-off controls with initial state $|0\rangle$ and target state $|1\rangle$. Two time-optimal controls are indicated by two blue pentagrams with $[t_1, t_2] = \{[T_1, T_2], [T_2, T_1]\}$.

small. In addition, the need of calculation of gradient makes the gradient-based algorithms less favorable. One of the disadvantages of SD is it usually converges slowly, thus requires large number of iterations.

D. Scheme

Specifically, for the first class of bang-off controls, we start from $N_s = 1$, and look through all possible types. For each type we optimize using SD the vector of durations \mathbf{t} for different values of total duration T , until the perfect fidelity $F = 1 - \delta$ is found, where $\delta \leq 10^{-8}$ is vanishingly small. We denote T_i^{\min} the minimal duration for which the perfect fidelity $F = 1 - \delta$ is obtained with number of switches being $N_s = i$. If $T_i^{\min} \approx T_{i+1}^{\min}$ and it is zero that one duration of optimized duration vector \mathbf{t} with $N_s = i + 1$, then this means the increment of number of switches does not decrease the minimal duration to reach perfect fidelity. Hence we can stop optimization and choose the types corresponding perfect fidelity with optimized \mathbf{t} and $N_s = i$ as the estimation of time-optimal control, and T_i^{\min} as the estimation of QSL.

For the second class, we optimize the control vectors using 1-flip SD. Here 1-flip means that the new candidates are generated by randomly choosing *one* time-slot and changing the value of control at that time-slot to other values [29].

In Ref. [18] it has been proved, for initial state $|0\rangle$ and target state $|1\rangle$ with $\alpha > \pi/4$, the time-optimal controls are first class of bang-off controls with one switch $N_s = 1$, i.e., $\{P_{T_1}N_{T_2}, P_{T_2}N_{T_1}, N_{T_1}P_{T_2}, N_{T_2}P_{T_1}\}$, where $T_1 = (\pi - \arccos(\cot^2 \alpha))/2\sqrt{E^2 + M^2} = 0.6505$ and $T_2 = (\pi + \arccos(\cot^2 \alpha))/2\sqrt{E^2 + M^2} = 1.2345$. Thus the quantum speed limit is $T_{\text{QSL}} = T_1 + T_2 = \pi/\sqrt{E^2 + M^2} = 0.6\pi$.

We wish to numerically estimate T_{QSL} and to obtain the time-optimal control field using the scheme proposed. We first investigate the first class with $N_s = 1$, and show that the minimal duration for perfect fidelity is equal to T_{QSL} . Then we show the bang-off controls with $N_s = 2$ reduce to the ones with $N_s = 1$ for the time-optimal problem considered here. At last, we consider the second class of bang-off controls, and compare the results between two classes.

A. First class with $N_s = 1$

We start from the first class of bang-off controls with $N_s = 1$. For the transition from $|0\rangle$ to $|1\rangle$, the number of possible types is two, i.e., $\{P_{t_1}N_{t_2}, N_{t_1}P_{t_2}\}$.

In Fig.1 we show the quantum control landscape for type $P_{t_1}N_{t_2}$. The control fields are characterized by a two-dimensional vector of durations $\mathbf{t} = [t_1, t_2]$. A similar landscape is obtained for type $N_{t_1}P_{t_2}$. The repetition of landscape over the square domain with time length T_{QSL} is because the time evolution of quantum state is periodic. In Fig.1 no local traps exist, while it is not true for the second class of bang-off controls. This is one of the advantages of the first class over the second one.

We now estimate the minimal duration T_i^{\min} for which the perfect fidelity $F = 1 - \delta$ is obtained. The procedure is in the following: choose different values of T with $t_1 + t_2 = T$; optimize the free variable t_1 using SD to maximize (minimize) fidelity F (Bures distance d_B). When $T \neq kT_{\text{QSL}}, k = 1, 2, \dots$ we find that d_B does not converge to zero. In addition, the optimization stops within fewer iterations when T deviates more from T_{QSL} . When $T = T_{\text{QSL}}$, however, d_B keeps decreasing and the update of control fields continues for a large number of iterations.

In Fig. 2(a)-(e) we show the Bures distance as a function of iteration for type $P_{t_1}N_{t_2}$ with five different values of T . One hundred initial search points of t_1 are randomly generated, and are optimized using SD. We find that as T approaches toward T_{QSL} , the convergence rate decreases, cf. Fig. 2(f). Moreover, the minimal Bures distance obtained after optimization decreases as T approaches toward T_{QSL} . When $T = T_{\text{QSL}}$, the Bures distance as a function hardly converge even for very large number of iterations. Therefore, we could estimate T_{QSL} by monitoring the convergence of Bures distance as an alternative method. For instance, in Fig. 2(c)

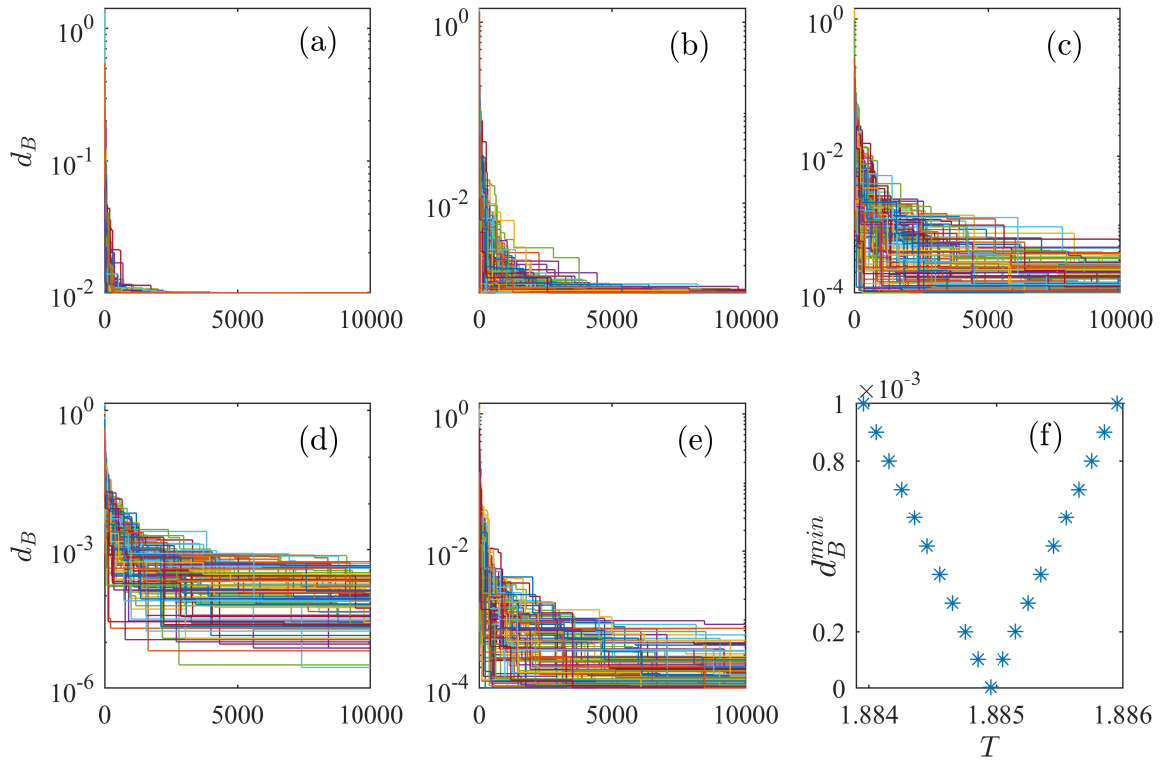


FIG. 2. Bures distance d_B versus iterations for different values of total evolution duration T : (a) $T = T_{\text{QSL}} - 10^{-2}$; (b) $T = T_{\text{QSL}} - 10^{-3}$; (c) $T = T_{\text{QSL}} - 10^{-4}$; (d) $T = T_{\text{QSL}}$; (e) $T = T_{\text{QSL}} + 10^{-4}$. The type of bang-off control is $P_{t_1}N_{t_2}$ with initial state $|0\rangle$ and target state $|1\rangle$, and the optimization algorithm is SD. The number of initial search points is one hundred, and the number of iteration is ten thousand. (f) The minimal d_B^{min} obtained after 10000 iterations for different values of total duration T . When $T = T_{\text{QSL}}$, the sequence of d_B^{min} reaches its minimum.

$T = T_{\text{QSL}} - 10^{-4}$, the search point with the minimal d_B found in the last iteration stops decreasing after several hundred iteration. For $T = T_{\text{QSL}}$, however, the optimization continues after ten thousand iterations, as shown in Fig. 2(d). Therefore, the minimal duration with one switch is approximately equal to the quantum speed limit $T_1^{\text{min}} = T_{\text{QSL}}$ with very high precision. In Fig. 2(d) 100 optimized values of t_1 cluster around T_1 and T_2 with significantly small standard deviation $\sigma \sim \mathcal{O}(10^{-4})$. The best fidelity (Bures distance) obtained after 10000 iterations is $F = 1 - 7.66 \times 10^{-12}$ ($d_B = 2.77 \times 10^{-6}$). Same results are obtained for type $N_{t_1}P_{t_2}$. Therefore the numerical results reproduce the analytical solutions with very high accuracy.

From the experimental point of view, the errors arise due to the operational inaccuracy. Therefore, we investigate the robustness of time-optimal bang-off controls with respect to small changes in the time vector \mathbf{t} . Random time vectors are drawn from a Gaussian distribution with the optimal values being the mean $[t_1 - T_1, t_2 - T_2] \sim \mathcal{N}(0, \sigma^2)$, where σ is the standard deviation. We sample 10000 time vectors and calculate the corresponding fidelity F for different values of σ . In Fig. 3 we show the mean E_m and standard deviation of

error distribution $E = 1 - F$. The mean of E is roughly a constant multiply the square of σ . Same for standard deviation of E . For instance, both mean and standard deviation are of the order of $\mathcal{O}(10^{-4})$ when $\sigma = 0.01$.

B. First class with $N_s = 2$

To numerically verify that the time-optimal controls are indeed of type with $N_s = 1$ for the case considered in this section, we continue to study the first class of bang-off controls with $N_s = 2$. We would show that $T_2^{\text{min}} = T_1^{\text{min}}$ with high precision, and one of three durations is zero, thus controls with $N_s = 2$ reduce to the ones with $N_s = 1$.

Specifically, for the transition from $|0\rangle$ to $|1\rangle$, the number of possible types is six, i.e., $\{P_{t_1}0_{t_2}N_{t_3}, N_{t_1}0_{t_2}P_{t_3}, P_{t_1}N_{t_2}P_{t_3}, N_{t_1}P_{t_2}N_{t_3}, P_{t_1}0_{t_2}P_{t_3}, N_{t_1}0_{t_2}N_{t_3}\}$. For the first four types, the perfect fidelity are reached when $T = T_{\text{QSL}}$, and one of the durations is zero, e.g., $t_2 = 0$ for $P_{t_1}0_{t_2}N_{t_3}$. For the last two types, the maximal fidelity is $F = 0.6399$ when $T = T_{\text{QSL}}$. When $T < T_{\text{QSL}}$, the perfect fidelity cannot be reached

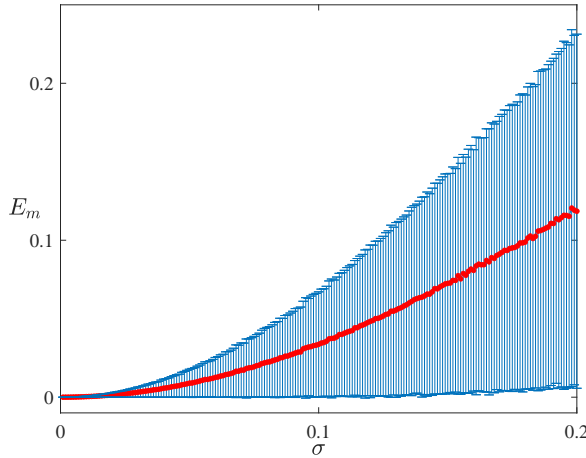


FIG. 3. Mean value E_m (red dots) of error distribution of $E = 1 - F$ as a function of σ using 10000 random time vectors \mathbf{t} drawn from Gaussian distribution with mean $[T_1, T_2]$ and standard deviation σ . The vertical blue lines represents the standard deviation of E .

for all six types. For instance, the maximal fidelity with $T = T_{\text{QSL}} - 0.001$ is $F = 1 - 1.001 \times 10^{-6}$ for type $P_{t_1} 0_{t_2} N_{t_3}$. Similar results are obtained for other types. Therefore, we have numerically verified that $T_2^{\min} = T_1^{\min} = T_{\text{QSL}}$.

In Fig. 4 we show the quantum control landscape for type $P_{t_1} 0_{t_2} N_{t_3}$ with $t_1 + t_2 + t_3 = T_{\text{QSL}}$. Two time-optimal controls are indicated by two pentagrams with $[t_1, t_2] = \{[T_1, 0], [T_2, 0]\}$. The duration for off-control $\omega(t) = 0$ is zero $t_2 = 0$, thus controls with $N_s = 2$ reduce to the ones with $N_s = 1$. We can observe the dark-red *U-shape* plateau of control landscape. Such plateaus make, in general, the optimizations fail to find the global optimal value, especially for the gradient-based algorithms.

We optimize the time vector $\mathbf{t} = [t_1, t_2]$ for type $P_{t_1} 0_{t_2} N_{t_3}$ with $t_3 = T_{\text{QSL}} - t_1 - t_2$ using SD with 100 initial search points and 10^6 iterations. The optimized time vector with the maximal fidelity $F = 1 - 1.24 \times 10^{-11}$ is $\mathbf{t} = [1.2253, 0.0181, 0.6415]$, while one of the optimal values is $\mathbf{t}_{\text{Opt}} = [T_2, 0, T_1] = [1.2345, 0, 0.6505]$. The Euclidean distance between these two time vectors is $\|\mathbf{t} - \mathbf{t}_{\text{Opt}}\|_2 = 0.023$. The deviation from the optimal value results from the flatness of U-shape plateau of landscape. In Fig. 4 we show the optimization process of one search point with best performance which climbs towards one of the optimal time vector. As search point is climbing towards the global maximum, smaller step-size and more iterations are required for better performance. Similar results are obtained for types $\{N_{t_1} 0_{t_2} P_{t_3}, P_{t_1} N_{t_2} P_{t_3}, N_{t_1} P_{t_2} N_{t_3}\}$.

The increment of switch numbers $N_s = 1 \rightarrow N_s = 2$ does not result in the decrement of total duration, but

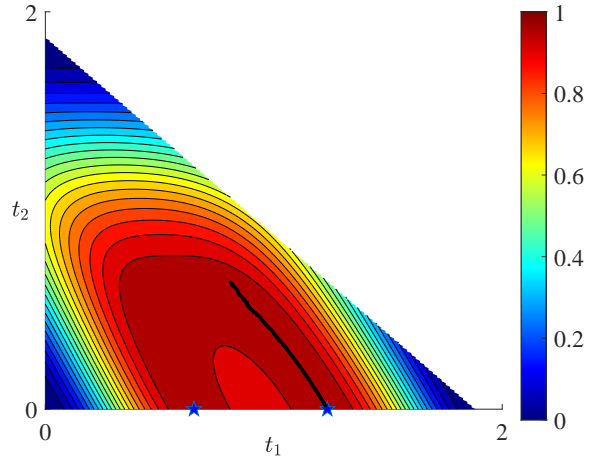


FIG. 4. Quantum control landscape of fidelity F for type $P_{t_1} 0_{t_2} N_{t_3}$ with initial state $|0\rangle$ and target state $|1\rangle$, and $t_1 + t_2 + t_3 = T_{\text{QSL}}$. Two time-optimal controls are indicated by two pentagrams for which $[t_1, t_2] = \{[T_1, 0], [T_2, 0]\}$. The black dots indicate the optimization process of one search point which climbs towards one of optimal time vector $\mathbf{t}_{\text{Opt}} = [T_2, 0]$ with the global maximum of fidelity $F = 1$.

$T_2^{\min} = T_1^{\min} = T_{\text{QSL}}$. In addition, we have shown that one duration of the optimized time vector is approximately equal to zero, thus the controls with $N_s = 2$ reduce to the ones with $N_s = 1$. Then we can stop studying the controls with larger number of switches $N_s \geq 3$.

In summary we have numerically verified for the transition $|0\rangle \rightarrow |1\rangle$ the time-optimal controls are $\{P_{T_1} N_{T_2}, P_{T_2} N_{T_1}, N_{T_1} P_{T_2}, N_{T_2} P_{T_1}\}$, and the quantum speed limit is T_{QSL} , with little deviations.

C. Second class of bang-off control

In this sub-section we consider the second class of bang-off controls as a comparison. Here we employ the 1-flip SD to optimize the control vectors where each component is allowed to take one of three values $\omega_k = \{\pm M, 0\}$. The number of time slots is fixed to be $N_T = 40$. 1000 initial control vectors are randomly generated and are optimized using SD for 10^4 iterations. To further investigate the relations between the optimized control fields, we calculate the distance between optimized control fields as

$$D_{ij} = \frac{1}{N_T} \|\omega^{(i)} - \omega^{(j)}\|_1 \quad (5)$$

where $\omega^{(i)}$ is the i -th optimized control field and $\|\cdot\|_1$ is the absolute-value norm [31].

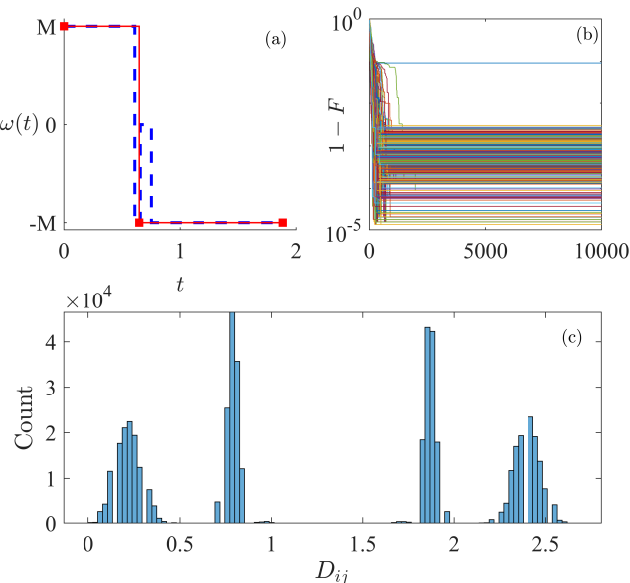


FIG. 5. The results obtained for transition from $|0\rangle$ to $|1\rangle$ using 1-flip SD to optimize the second class of bang-off controls. The number of time slots is fixed to be $N_T = 40$. (a) The optimized bang-off control with maximal fidelity found by 1-flip SD (blue, dashed) and one of the time-optimal controls (red, solid) $P_{T_1}N_{T_2}$. (b) Infidelity $1-F$ versus iterations with 1000 search points. (c) Distribution of distance D_{ij} between optimized control fields.

In Fig. 5 we demonstrate the results found by 1-flip SD with total duration $T = \tau_{\text{QSL}}$. In Fig. 5(a) the optimized control field found with maximal fidelity found is indicated by the blue dashed line, while one of the time-optimal control fields $P_{T_1}N_{T_2}$ is marked by the red solid line. We can observe that the temporal shape of the optimized control field found by 1-flip is similar to that of time-optimal control $P_{T_1}N_{T_2}$, but the number of switch is three. In Fig. 5(b) we plot the infidelity $1-F$ as a function of optimization iteration. 1-flip SD stops updating after about 1000 iterations, and the maximal fidelity obtained is $F = 1 - 1.35 \times 10^{-5}$. Presumably, the performance of second class of bang-off controls would be improved by k -flip SD ($k \geq 2$), yet the number of iterations required is much larger [29]. In Fig. 5(c) distances between optimized control fields D_{ij} form a multimodal distribution with four peaks. This yields the fact that the optimized control fields cluster around four time-optimal controls $\{P_{T_1}N_{T_2}, P_{T_2}N_{T_1}, N_{T_1}P_{T_2}, N_{T_2}P_{T_1}\}$ with a standard deviation much larger than that obtained with first class of bang-off controls.

Therefore, for the time-optimal problem of quantum transition from $|0\rangle$ to $|1\rangle$, the performance of first class of bang-off control is better than that of second class using 1-flip SD, concerning the maximal fidelity obtained, the optimized control fields found and the their distribution.

IV. TRANSITION FROM $|0\rangle$ TO $|\psi_E\rangle$

In this section we consider the transition from $|0\rangle$ to $|\psi_E\rangle$ with $\alpha > \pi/4$. The time-optimal controls are of first class bang-off controls with two switches $N_s = 2$: $\{P_{T_1}0_{T_2}N_{T_3}, P_{T_1}0_{T_2}P_{T_3}\}$ [18]. Three durations are: $\tau_1 = T_1 = 0.6505$ is the duration for which the time-evolving quantum state reaches the equator of Bloch sphere for the first time under the control field $\omega(t) = M$. The quantum state after this process is $|A^+\rangle = 1/\sqrt{2}(|0\rangle + e^{i(\pi+\beta)}|1\rangle)$ (up to a global phase) with $\beta = \arccos E/M = 0.7227$; $\tau_2 = (\beta - \pi/10)/2E = 0.2043$ is the duration for which the quantum state reaches $|\psi'_E\rangle = 1/\sqrt{2}(|0\rangle + e^{i11\pi/10}|1\rangle)$ along the equator starting from $|A^+\rangle$ with the control field $\omega(t) = 0$; and $\tau_3 = 0.2978$ is the duration for which the quantum state reaches target state $|\psi_E\rangle$ from $|\psi'_E\rangle$ with the control fields $\omega(t) = \pm M$. The quantum speed limit is $\tau_{\text{QSL}} = \tau_1 + \tau_2 + \tau_3 = 1.1525$. Here we use a different notation τ_{QSL} for QSL to distinguish it from the one in Sec. III.

A. First class with $N_s = 1$

For the transition considered in this section, the possible types of first class are four: $\{P_{T_1}0_{T_2}, P_{T_1}N_{T_2}, N_{T_1}0_{T_2}, N_{T_1}P_{T_2}\}$. When $T = \tau_{\text{QSL}}$, the maximal fidelity of four types are: $F = [0.9997, 1 - 5.0937 \times 10^{-6}, 0.4999, 0.9873]$. Therefore, the time-optimal controls cannot be the ones with $N_s = 1$ because $T_1^{\min} > \tau_{\text{QSL}}$. It is worth noting that although $T_1^{\min} > \tau_{\text{QSL}}$, the perfect fidelity can be obtained using $N_s = 1$ controls with a larger duration, e.g., $P_{T_1}0_\lambda$ with $\lambda = \beta + \pi/10 = 0.5184$ and the total duration $T = \tau_1 + \lambda = 1.1689$ which is a little larger than $\tau_{\text{QSL}} = 1.1525$. Because of the operational inaccuracy in experiment, the larger N_s is, the larger the error is. Therefore, the controls with $N_s = 1$ is acceptable, provided the perfect fidelity can be obtained and the total duration which does not exceed τ_{QSL} much is tolerable.

B. First class with $N_s = 2$

We could estimate T_2^{\min} using the same scenario in Sec. III. An alternative method is to calculate the fidelity for time vectors in the fine-grained 3D temporal space. Find the locations of perfect fidelity and choose the shortest duration as the estimate of T_2^{\min} .

In Fig. 6 we show the quantum control landscape of fidelity for $P_{T_1}0_{T_2}N_{T_3}$ with $t_1 + t_2 + t_3 = \tau_{\text{QSL}}$. The perfect fidelity is indicated by a blue pentagram with the optimal time vector $\mathbf{t}_{\text{opt}} = [\tau_1, \tau_2, \tau_3] = [0.6505, 0.2043, 0.2978]$. By investigating the landscape with durations $T < \tau_{\text{QSL}}$, perfect fidelity cannot be reached. It is interesting to notice that there is only one maximum, which is also the

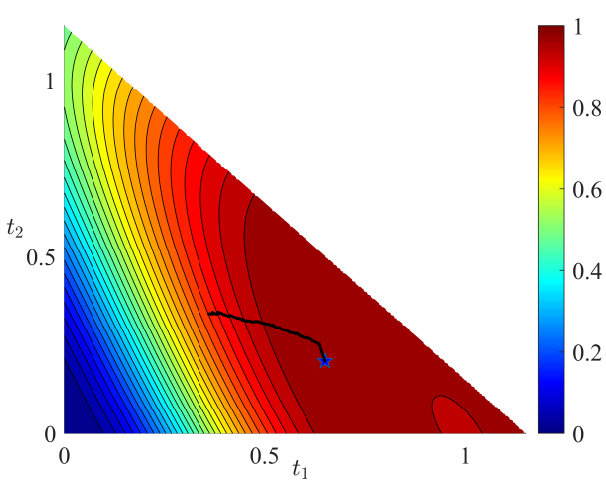


FIG. 6. Quantum control landscape of fidelity F for type $P_{t_1} 0_{t_2} N_{t_3}$ with initial state $|0\rangle$ and target state $|\psi_E\rangle$, and $t_1 + t_2 + t_3 = \tau_{QSL}$. The time-optimal control is indicated by a blue pentagram with $\tau_{\text{Opt}} = [\tau_1, \tau_2]$. The black dots indicate the optimization process of one search point which climbs towards one of optimal time vector \mathbf{t}_{Opt} with the global maximum of fidelity $F = 1$.

global maximum, in the landscape of fidelity. Therefore, all search points should converge towards the optimal time vector, and indeed this is true in our numerical optimization process. 100 search points are optimized using SD, and the maximal fidelity obtained after 10^6 iterations is $F = 1 - 2.220 \times 10^{-16}$. The optimized time vector is $\mathbf{t} = [0.6504, 0.2046, 0.2976]$. Therefore we numerically verified $T_2^{\min} = \tau_{QSL}$ with high accuracy.

We can observe flatness of landscape near the perfect fidelity in Fig. 6. This can be further verified through the optimization process. We notice that even though the Euclidean distance between the optimized time vector and the optimal time vector $\|\mathbf{t} - \mathbf{t}_{\text{Opt}}\|_2$ is of the order of 10^{-4} , the deviation from the perfect fidelity $1 - F$ is significantly small, i.e., of the order of 10^{-16} . Such flatness usually makes the gradient-based algorithms fails. Similar results are obtained for type $P_{t_1} 0_{t_2} P_{t_3}$.

One of the benefits using SD optimizing over first class of bang-off controls is that we could estimate the number of local extremes and their values, as well as the location of corresponding controls. For instance, in Fig. 7(a) we show the quantum control landscape of log-Bures distance $\log_{10}(d_B)$ for type $P_{t_1} N_{t_2} 0_{t_3}$ with $t_1 + t_2 + t_3 = \tau_{QSL}$. Note that perfect fidelity cannot be reached for type $P_{t_1} N_{t_2} 0_{t_3}$ with total duration being τ_{QSL} . Two local minima exist in the landscape, and are estimated by optimizing 100 search points which are randomly sampled in the beginning of optimization. It is clearly shown in Fig. 7(b) two branches of search points saturate towards different values of $\log_{10}(d_B)$. It is worth

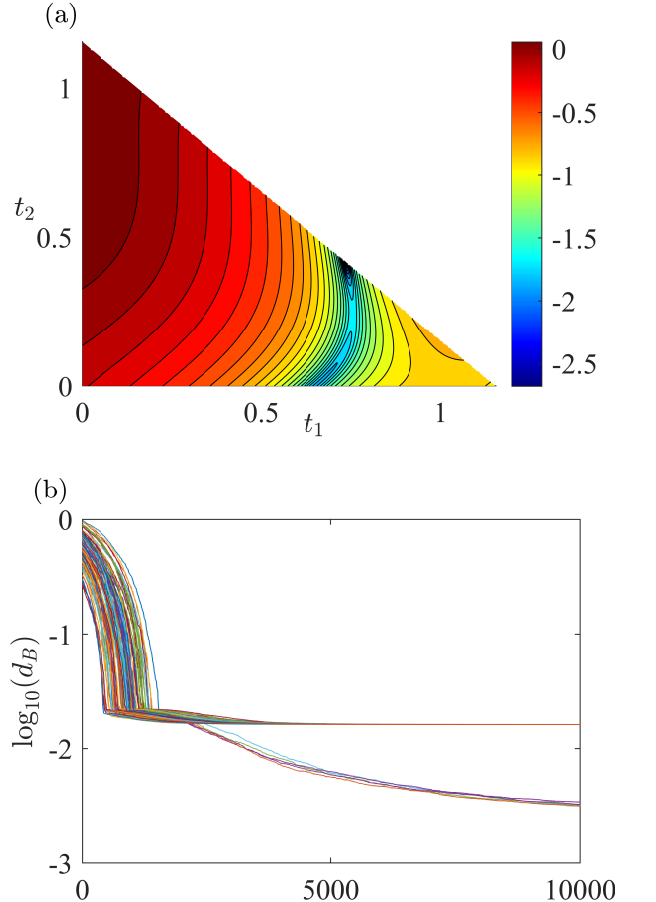


FIG. 7. (a) Quantum control landscape of log-Bures distance $\log_{10}(d_B)$ for type $P_{t_1} N_{t_2} 0_{t_3}$ with $t_1 + t_2 + t_3 = \tau_{QSL}$. Two local minima are shown with blue color. (b) $\log_{10}(d_B)$ as a function of optimization iteration with 100 initial search points. 100 search points saturated towards two branches with values of $\log_{10}(d_B)$ being $[-1.7916, -2.6825]$ after 10000 iterations.

noting that since the two local minima are far from each other, given that the step-size of optimization is small, it is hardly possible for search points to jump from one local trap to another. If the distance between two local minima is small, the search points might jump from one to another. Similar results are obtained for other types.

Therefore, we have estimated that $T_2^{\min} = \tau_{QSL}$ and the perfect fidelity is reached for control fields $\{P_{\tau_1} 0_{\tau_2} N_{\tau_3}, P_{\tau_1} 0_{\tau_2} P_{\tau_3}\}$.

C. First class with $N_s = 3$

To further verify the time-optimal controls are of types with $N_s = 2$, we continue to study the first class bang-off controls with $N_s = 3$. For illustration, we consider the type $P_{t_1} 0_{t_2} N_{t_3} 0_{t_4}$. We would demonstrate that $T_3^{\min} =$

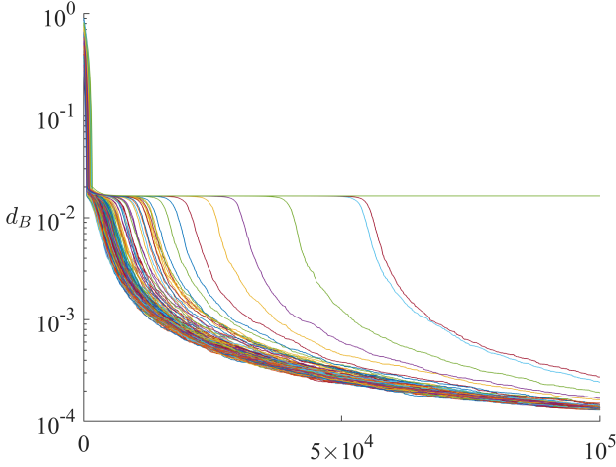


FIG. 8. Bures distance d_B versus iterations for type $P_{t_1} 0_{t_2} N_{t_3} 0_{t_4}$ with the total evolution duration $T = \tau_{\text{QSL}}$. 200 initial search points are optimized using SD with 10^5 iterations.

T_2^{\min} , and one of the durations is zero $t_4 = 0$.

By investigating the control landscape, we verify that the time vector corresponding the perfect fidelity with minimal duration is $\mathbf{t}_{\text{Opt}} = [\tau_1, \tau_2, \tau_3, 0]$ (data not shown). This is further confirmed by the optimization. 200 time vectors $\mathbf{t} = [t_1, t_2, t_3, t_4]$ are optimized using SD with $t_1 + t_2 + t_3 + t_4 = \tau_{\text{QSL}}$ for 10^5 iterations. In Fig. 8 we show Bures distance d_B as a function of iteration. It is interesting to notice from Fig. 8 that there are one local minimum and one global minimum of landscape, and they are not far from each other. Therefore, some of the search points are able to jump outside the local minimum and move towards the global one.

The minimal value obtained is $d_B = 1.29 \times 10^{-4}$, the corresponding fidelity is $F = 1 - 1.67 \times 10^{-8}$, and the optimized time vector is $\mathbf{t} = [0.6507, 0.2037, 0.2977, 4.064 \times 10^{-4}]$ with one duration being approximately equal to zero $t_4 \approx 0$. Similar results are obtained for type $\{P_{t_1} 0_{t_2} N_{t_3} P_{t_4}, P_{t_1} 0_{t_2} P_{t_3} 0_{t_4}, P_{t_1} 0_{t_2} P_{t_3} N_{t_4}\}$, while the perfect fidelity cannot be reached for other types with the total duration being τ_{QSL} . Therefore, we have numerically checked that $T_3^{\min} = T_2^{\min} = \tau_{\text{QSL}}$ with high accuracy, hence the optimal controls with $N_s = 3$ reduce to the ones with $N_s = 2$.

Considering that the optimal controls with $N_s = 3$ reduce to the ones with $N_s = 2$ and $T_3^{\min} = T_2^{\min}$, there is no need to study the first class of controls with larger switch numbers $N_s \geq 4$.

In summary we have numerically verified for the transition considered in this section the time-optimal controls are $\{P_{\tau_1} 0_{\tau_2} N_{\tau_3}, P_{\tau_1} 0_{\tau_2} P_{\tau_3}\}$, and the quantum speed limit

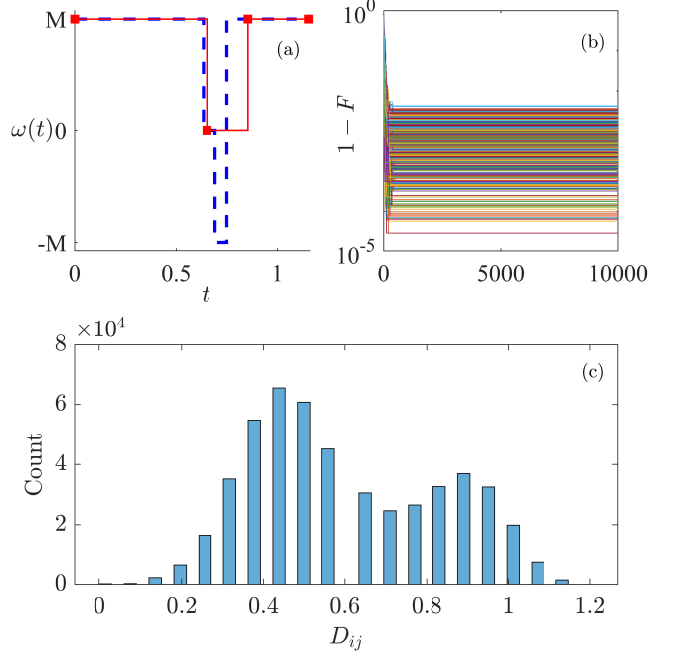


FIG. 9. The results obtained for transition from $|0\rangle$ to $|\psi_E\rangle$ using 1-flip SD optimizing the second class of bang-off controls with total duration being $T = \tau_{\text{QSL}}$. The number of time slots is fixed to be $N_T = 20$. (a) The optimized bang-off control with maximal fidelity found by 1-flip SD (blue, dashed) and one of the time-optimal controls (red, solid) $P_{\tau_1} 0_{\tau_2} P_{\tau_3}$. (b) Infidelity $1 - F$ versus iterations with 1000 search points. (c) Distribution of distance D_{ij} between optimized control fields.

is τ_{QSL} , with high precision.

D. Second class of bang-off control

Same as Sec. III we investigate the performance of the second class of bang-off controls using the 1-flip SD. 1000 initial control vectors are randomly generated and are optimized for 10^4 iterations with the number of time slots being $N_T = 20$. Distance between optimized control fields D_{ij} are calculated.

In Fig. 9 the results of optimization are shown with total duration $T = \tau_{\text{QSL}}$. In Fig. 9(a) one of the time-optimal control fields $P_{\tau_1} 0_{\tau_2} P_{\tau_3}$ is marked by the red solid line, and the optimized control field with maximal fidelity found is indicated by the blue dashed line. The temporal shape of the optimized control field found by 1-flip SD is again similar to that of time-optimal control $P_{\tau_1} 0_{\tau_2} P_{\tau_3}$, except for certain duration the optimized control takes the value $\omega(t) = -M$, rather than the expected value $\omega(t) = 0$. In Fig. 9(b) we plot the infidelity $1 - F$ as a function of optimization iteration. 1-flip SD stops updating after about 100 iterations, and the maximal fidelity obtained is $F = 1 - 2.77 \times 10^{-6}$.

Hence the performance of second class of bang-off controls using 1-flip SD is not as good as the first class. In Fig. 9(c) distances between optimized control fields D_{ij} form a bimodal distribution, which indicates the optimized control fields cluster around two time-optimal controls $\{P_{\tau_1} 0_{\tau_2} P_{\tau_3}, P_{\tau_1} 0_{\tau_2} N_{\tau_3}\}$.

V. CONCLUSIONS

We have proposed a systematic scheme for numerically estimating the quantum speed limit and approximating the temporal shape of time-optimal control with bounded

amplitude. We have studied as examples the time-optimal control problem of two quantum state transition processes in two-level quantum system. Two classes of bang-off controls are optimized using stochastic descent algorithm, and the numerical results are compared to the analytic results. We find that the deviations from analytic solutions are significantly small. We have also investigated the robustness of first class of bang-off controls. In addition, the performance of first class is better than that of second class concerning the fidelity obtained and the optimized control field found. It is interesting to employ this scheme to high-dimensional quantum systems. This issue is left for future work.

[1] S. J. Glaser, U. Boscain, T. Calarco, C. P. Koch, W. Köckenberger, R. Kosloff, I. Kuprov, B. Luy, S. Schirmer, T. Schulte-Herbrüggen, D. Sugny, and F. K. Wilhelm, Training schrödinger's cat: quantum optimal control, *The European Physical Journal D* **69**, 279 (2015).

[2] D. D'Alessandro, *Introduction to Quantum Control and Dynamics* (2nd ed.) (Chapman and Hall/CRC, 2021).

[3] V. F. Krotov, Global methods in optimal control theory, in *Advances in Nonlinear Dynamics and Control: A Report from Russia*, edited by A. B. Kurzhanski (Birkhäuser Boston, Boston, MA, 1993) pp. 74–121.

[4] C. Brif, R. Chakrabarti, and H. Rabitz, Control of quantum phenomena: past, present and future, *New Journal of Physics* **12**, 075008 (2010).

[5] T. Gericke, F. Gerbier, A. Widera, S. Fölling, O. Mandel, and I. Bloch, Adiabatic loading of a bose-einstein condensate in a 3d optical lattice, *Journal of Modern Optics* **54**, 735 (2007), <https://doi.org/10.1080/09500340600777730>.

[6] D. Guéry-Odelin, A. Ruschhaupt, A. Kiely, E. Torrontegui, S. Martínez-Garaot, and J. G. Muga, Shortcuts to adiabaticity: Concepts, methods, and applications, *Rev. Mod. Phys.* **91**, 045001 (2019).

[7] X. Chen, A. Ruschhaupt, S. Schmidt, A. del Campo, D. Guéry-Odelin, and J. G. Muga, Fast optimal frictionless atom cooling in harmonic traps: Shortcut to adiabaticity, *Phys. Rev. Lett.* **104**, 063002 (2010).

[8] S. van Frank, M. Bonneau, J. Schmiedmayer, S. Hild, C. Gross, M. Cheneau, I. Bloch, T. Pichler, A. Negretti, T. Calarco, and S. Montangero, Optimal control of complex atomic quantum systems, *Scientific Reports* **6**, 34187 (2016).

[9] N. Khaneja, T. Reiss, C. Kehlet, T. Schulte-Herbrüggen, and S. J. Glaser, Optimal control of coupled spin dynamics: design of nmr pulse sequences by gradient ascent algorithms, *Journal of Magnetic Resonance* **172**, 296 (2005).

[10] X. Li, D. Pecak, T. Sowiński, J. Sherson, and A. E. B. Nielsen, Global optimization for quantum dynamics of few-fermion systems, *Phys. Rev. A* **97**, 033602 (2018).

[11] N. S. Srivatsa, X. Li, and A. E. B. Nielsen, Squeezing anyons for braiding on small lattices, *Phys. Rev. Research* **3**, 033044 (2021).

[12] T. Caneva, M. Murphy, T. Calarco, R. Fazio, S. Montangero, V. Giovannetti, and G. E. Santoro, Optimal control at the quantum speed limit, *Phys. Rev. Lett.* **103**, 240501 (2009).

[13] S. Lloyd and S. Montangero, Information theoretical analysis of quantum optimal control, *Phys. Rev. Lett.* **113**, 010502 (2014).

[14] D. D'Alessandro and M. Dahleh, Optimal control of two-level quantum systems, *IEEE Transactions on Automatic Control* **46**, 866 (2001).

[15] U. Boscain, G. Charlot, J.-P. Gauthier, S. Guérin, and H.-R. Jauslin, Optimal control in laser-induced population transfer for two- and three-level quantum systems, *Journal of Mathematical Physics* **43**, 2107 (2002), <https://aip.scitation.org/doi/pdf/10.1063/1.1465516>.

[16] N. Khaneja, R. Brockett, and S. J. Glaser, Time optimal control in spin systems, *Phys. Rev. A* **63**, 032308 (2001).

[17] U. Boscain and Y. Chitour, Time-optimal synthesis for left-invariant control systems on $so(3)$, *SIAM Journal on Control and Optimization* **44**, 111 (2005), <https://doi.org/10.1137/S0363012904441532>.

[18] U. Boscain and P. Mason, Time minimal trajectories for a spin 1/2 particle in a magnetic field, *Journal of Mathematical Physics* **47**, 062101 (2006), <https://doi.org/10.1063/1.2203236>.

[19] U. Boscain, F. Grönberg, R. Long, and H. Rabitz, Minimal time trajectories for two-level quantum systems with two bounded controls, *Journal of Mathematical Physics* **55**, 062106 (2014), <https://doi.org/10.1063/1.4882158>.

[20] G. C. Hegerfeldt, Driving at the quantum speed limit: Optimal control of a two-level system, *Phys. Rev. Lett.* **111**, 260501 (2013).

[21] G. C. Hegerfeldt, High-speed driving of a two-level system, *Phys. Rev. A* **90**, 032110 (2014).

[22] A. D. Boozer, Time-optimal synthesis of $su(2)$ transformations for a spin-1/2 system, *Phys. Rev. A* **85**, 012317 (2012).

[23] M. Jafarizadeh, F. Naghdi, and M. Bazrafkan, Time optimal control of two-level quantum systems, *Physics Letters A* **384**, 126743 (2020).

[24] S. E. Sklarz and D. J. Tannor, Loading a bose-einstein condensate onto an optical lattice: An application of optimal control theory to the nonlinear schrödinger equation, *Phys. Rev. A* **66**, 053619 (2002).

- [25] P. Doria, T. Calarco, and S. Montangero, Optimal control technique for many-body quantum dynamics, *Phys. Rev. Lett.* **106**, 190501 (2011).
- [26] J. J. W. H. Sørensen, M. O. Aranburu, T. Heinzel, and J. F. Sherson, Quantum optimal control in a chopped basis: Applications in control of bose-einstein condensates, *Phys. Rev. A* **98**, 022119 (2018).
- [27] S. Machnes, E. Assémat, D. Tannor, and F. K. Wilhelm, Tunable, flexible, and efficient optimization of control pulses for practical qubits, *Phys. Rev. Lett.* **120**, 150401 (2018).
- [28] E. Zahedinejad, S. Schirmer, and B. C. Sanders, Evolutionary algorithms for hard quantum control, *Phys. Rev. A* **90**, 032310 (2014).
- [29] M. Bukov, A. G. R. Day, D. Sels, P. Weinberg, A. Polkovnikov, and P. Mehta, Reinforcement learning in different phases of quantum control, *Phys. Rev. X* **8**, 031086 (2018).
- [30] A. N. Pechen and D. J. Tannor, Are there traps in quantum control landscapes?, *Phys. Rev. Lett.* **106**, 120402 (2011).
- [31] M. Larocca, P. M. Poggi, and D. A. Wisniacki, Quantum control landscape for a two-level system near the quantum speed limit, *Journal of Physics A: Mathematical and Theoretical* **51**, 385305 (2018).